

Spatial heterogeneity of soil nitrogen in a subtropical forest in China

Lixin Wang · Paul P. Mou · Jianhui Huang · Jin Wang

Received: 9 January 2007 / Accepted: 10 April 2007 / Published online: 10 May 2007
© Springer Science+Business Media B.V. 2007

Abstract Spatial variability of soil total nitrogen (N), available N (KCl extractable NH_4^+ and NO_3^-), and spatial patterns of N mineralization and nitrification at a stand scale were characterized with geostatistical and univariate analysis. Two extensive soil spatial samplings were conducted in an evergreen broadleaf forest in Sichuan province, southwestern China in June and August 2000. In a study area of $90 \times 105 \text{ m}^2$, three soil samples were collected from each $5 \times 5 \text{ m}^2$ plot ($n = 378$) in June and August, and were analyzed for total N and available N contents. Net N mineralization and nitrification were measured by in situ core incubation and the rates were estimated based on the

difference of NH_4^+ and NO_3^- contents between the two sampling dates. Total N, NH_4^+ and NO_3^- were all spatially structured with different semivariogram ranges (from high to low: NH_4^+ , NO_3^- , and total N). The semivariograms of mineralization and nitrification were not as spatially structured as available N. NH_4^+ was the dominant soil inorganic N form in the system. Both NH_4^+ and NO_3^- affected spatial patterns of soil available N, but their relative importance switched in August, probably due to high nitrification as indicated by greatly increased soil NO_3^- content. High spatial auto-correlations (>0.7) were found between available N and NH_4^+ available N and NO_3^- on both sampling dates, as well as total N measurements between both sampling dates. Although significant, the spatial auto-correlation between NH_4^+ and NO_3^- were generally low. Topography had significant but low correlations with mineralization ($r = -0.16$) and nitrification ($r = -0.14$), while soil moisture did not. The large nugget values of the calculated semivariograms and high-semivariance values, particularly for mineralization and nitrification, indicate that some fine scale ($<5 \text{ m}$) variability may lie below the threshold for detection in this study.

L. Wang · J. Huang (✉) · J. Wang
Laboratory of Quantitative Vegetation Ecology, Institute of Botany, The Chinese Academy of Sciences, Beijing 100093, China
e-mail: jhhuang@ibcas.ac.cn

L. Wang · J. Wang
Department of Environmental Sciences, University of Virginia, Charlottesville, VA 22904, USA

L. Wang
e-mail: Lixin@virginia.edu

J. Wang
e-mail: Jw2dy@virginia.edu

P. P. Mou
College of Life Sciences, Beijing Normal University, Beijing 100875, China
e-mail: ppmou@uncg.edu

Keywords Available N · Heterogeneity · Spatial pattern · Total N

Introduction

As the most limiting nutrient element in many forest ecosystems, including boreal and temperate forests, nitrogen (N) availability constrains ecosystem productivity (Aber et al. 1989; Rastetter et al. 1997; Reich et al. 2006), and affects biogeochemical cycles of other elements mainly through the process of litter decomposition (Tamm 1991). Soil is the primary and most immediate N pool for plants and microbes in forested ecosystems (Kimmins 2004). The soil chemical and physical features within an ecosystem are highly heterogeneous in space (Brady and Weil 1999). Soil heterogeneity inevitably affects local N pools and complex soil processes governing N cycling (Perez et al. 1999). As a consequence, soil N availability can be spatiotemporally heterogeneous, influencing local plants and community development (Mou et al. 1993a, 2005; Hutchings et al. 2003; Wijesinghe et al. 2005). There have been reports that soil N heterogeneity influences seedling recruitment (Mou et al. 1993b), plant species coexistence, competition (Gallardo et al. 2000), and vegetation succession (Gross et al. 1995). Recent studies also suggest that changes in N heterogeneity affected invasion of non-native plants into natural ecosystems (Siemann and Rogers 2003; Cassidy et al. 2004).

Available N, primarily ammonium (NH_4^+) and nitrate (NO_3^-) have been frequently observed to be variable in both space and time in different ecosystems (Hammer et al. 1987; Garten et al. 1994; Lovett and Rueth 1999). Spatial patterns of NH_4^+ and NO_3^- , however, are less well characterized (Lister et al. 2000; Gallardo et al. 2005) and results reported in the literature are mixed. Some found that both soil NH_4^+ and NO_3^- were spatially structured and NH_4^+ had higher semivariogram range than NO_3^- (Gross et al. 1995; Gallardo et al. 2005), while others revealed spatial structure for NO_3^- but not for NH_4^+ (Cain et al. 1999; Lister et al. 2000). There is still little knowledge about the spatial patterns of N mineralization and nitrification (Morris and Boerner 1998; Smithwick et al. 2005b), especially at ecosystem scale, probably due to the required high intensity of field sampling (Jackson and Caldwell 1993; Gross et al. 1995). In addition, although it is clear that in most mature undisturbed temperate forests the soil inorganic N pools are dominated by ammonium (Kronzucker et al. 1997), the question remains unanswered

how the spatial variations of NH_4^+ and NO_3^- and their temporal changes contribute to the spatial variation of the total inorganic N pool. Comprehension of spatiotemporal patterns of soil available N will be of great significance in a more thorough understanding of vegetation dynamics, productivity, and ecosystem functions at different spatiotemporal scales (Cwiling and Field 2003; Lane and Bassiriraj 2005).

Therefore, studies that feature intensive collecting of spatial data from different ecosystems are essential.

We conducted a study in a mature secondary evergreen broadleaf forest in western Sichuan province, southwestern China to survey the spatial variation of total soil N and available soil N. We then used the data sets to calculate the spatial variations of N mineralization and nitrification. Soils in trough topographic location are usually deeper with higher soil moisture condition. Higher soil moisture may facilitate N mineralization and nitrification (Burke 1989; Verchot et al. 2002). We acquired the topographic data and the spatial data on soil moisture to examine their possible effects on the spatial patterns of the different N forms. The objectives of this study are: (1) to determine the spatial structure of NH_4^+ , NO_3^- , and N mineralization and nitrification in a subtropical evergreen forest at the ecosystem level; (2) to determine how they are spatially correlated and how they were affected by spatial environmental variation such as topography and soil water conditions. We expect that (1) NH_4^+ , NO_3^- , and N mineralization and nitrification are spatially structured and affected by local topography and soil water content; and (2) these spatial patterns are highly correlated due to their close biogeochemical links. We chose the subtropical evergreen forests because (1) information is generally lacking on N mineralization and nitrification in subtropical forest ecosystems (Maithani et al. 1998; Upadhyaya et al. 2005); and (2) subtropical forests in southwestern China have been threatened by human activities. Many are isolated and fragmented by deforestation and other socio-economic developments (Chen 2000a). This study of the spatiotemporal dynamics of N patterns will not only provide insights into N cycling in these ecosystems, but also provide information for natural ecosystem restoration and forest management in the region, where N is considered to be a limiting factor for plant uptake (Wang et al. unpublished data).

Materials and methods

Site description

The study site is a naturally regenerated secondary evergreen broadleaf forest (90 years) near Dujiangyan city, Sichuan province, southwest China (30°44' N, 103°27' E) on the east slope of the east rim of the Tibetan Plateau. The elevation of the study site is between 755 and 805 m above the sea level with a narrow valley (trough feature) in the middle of the study site. The general slope aspect is south-facing and the average slope is about 30°. It has a typical subtropical monsoon climate with cool, dry winters from December to February and humid, warm summers from May to October. The mean annual temperature is 15.2°C with a mean January temperature of 4.6°C, and a mean July temperature of 24.9°C. The mean annual precipitation is 1,200–1,500 mm, most of which falls in the summer from June to September. Influenced by the Pacific monsoon from the southeast, the orographic precipitation dominates the region (Chen 2000a). The soil type is classified as mountain brown yellow soil (equivalent to a US Soil Taxonomy Ultisols) according to the Chinese Soil Classification System (Chen 2000b) with little litter accumulation. The canopy is dominated by *Castanopsis fargesii* Franch. The other abundant species include *Cyclobalanopsis glauca* (Thunb.) Oerst., *Machilus pingii* Cheng ex Yang, and *Symplocos laurina* (Retz.) Wall. The important understory species are *Camellia oleifera* Obel., *Lindera pulcherrima* (Wall.) Benth., *Ilex szechwanensis* Loes., *Pittosporum sahnianum* Gowda, and *Bambusa omeiensis* Chia and H. L. Fung. The ground-level was dominated by ferns, including *Microlepia marginata* (Houtt.) C. Chr., and *Trachinodes rhomboidea* (Wall.) Ching.

A survey site of 90 × 105 m² was established in the middle of the forest in June 2000. The site was fenced to avoid external disturbances. Then, the study site was grided into 378 × 5 m² subplots (Fig. 1). The boundary of the study site was located by GPS and matched to a 1:10,000 topographic map. The elevation of each grid center was interpolated from the map. The relative topographic position (ridge, back slope, and foothill) of each grid was also determined from the map for examining relationships between measured N spatial variability and topography.

Soil sampling and chemical analyses

Net N mineralization and nitrification were measured with the in situ core incubation method following Raison et al. (1987). Three soil samples of top 15 cm were randomly taken in the central portion of each plot (total 1,134 samples) in June 2000 (Fig. 1). Each sample was taken by driving a PVC pipe of 5 cm in diameter and 15 cm in depth into the soil. After sampling from each plot, one PVC pipe of the same size was then inserted into the ground nearby (20–30 cm away) to start incubation. Three such pipes per plot were inserted for incubation. Each pipe was covered with a plastic film at the top to prevent rain water from entering, and with a 1 mm mesh net at the bottom to allow water, gas exchange, and soil microfauna to enter (Binkley and Hatfield 1989). To put the net at the bottom of a PVC pipe, we first took a soil sample out using a PVC pipe with soil remaining in the pipe. Then we attached mesh to the bottom of the pipe and inserted this pipe back into the hole left from taking that specific soil sample. All the incubated pipes were harvested in August 2000, and the soils inside were collected. All soil samples were stored in cloth bags, and processed in the field lab the same day.

The soil from each pipe was thoroughly mixed and air-dried in the field. The samples were then ground to pass a No. 10 sieve (mesh size 2 mm) after small plant parts and stones were removed. Each soil sample was subsampled (6 g) and extracted with 30 ml 1 M KCl solution for NH₄⁺ and NO₃⁻ analyses following the standard procedure (Maynard and Kalra 1993). The extracts were analyzed with a Segmented Flow Analyzer (Segmented Flow Analyzer, the scalar SAN^{plus}, Breda, The Netherlands). The remainder of each soil sample was ground to pass through a No. 100 sieve (mesh size 0.15 mm) and subsampled for Kjeldahl total N (%) analysis following standard procedure (Bremner 1996). Gravimetric moisture content was determined for 25 randomly selected samples at each sampling period using an oven-drying method (105°C) following Gardner (1986).

Calculation and data analysis

The soil analyses yielded three data sets for each of the June and August samplings: soil N content, NO₃⁻ content, and total N content. Adding N_{min} and

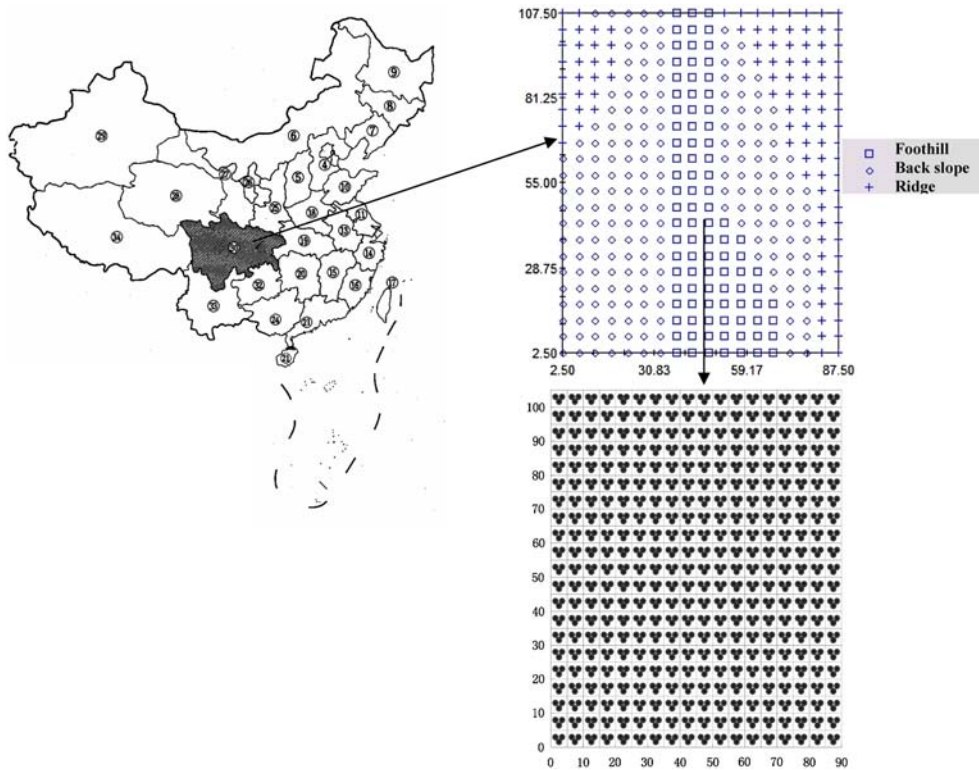


Fig. 1 Site location, topography (from 1:10,000 map), and diagram of sampling strategy. The shaded area is Sichuan province where the site was located. The small squares are 5 m². From

each small square, we took three soil samples in June and started to incubate another three samples in situ. These three samples were collected in August at the end of incubation

NO₃⁻ together yielded the soil available N data set. The values of the three samples from each 5 m² plot were averaged to represent each 5 m² plot.

The net N mineralization rate (R_M) (μg N/g/day) was evaluated by:

$$R_M = (C_{m1} - C_{m0})/T, \tag{1}$$

where C_{m1} and C_{m0} (μg N/g) represent final values and initial values of (NH₄⁺ + NO₃⁻), respectively. T represents the total days of incubation.

Similarly, the net nitrification rate (R_N) (μg N/g/day) was evaluated by:

$$R_N = (C_{n1} - C_{n0})/T, \tag{2}$$

where C_{n1} and C_{n0} (μg N/g) represent final values and initial values of NO₃⁻. T represents the total days of incubation (Raison et al. 1987).

To examine our expectations, we used both conventional statistics and geostatistics to analyze on the amount of auto-correlation in the data.

the spatial features of the measured variables. Conventional statistics were used to indicate the degree of overall variation, while geostatistics were used to examine whether or not a variable is spatially structured.

Data normality for all data sets was tested (SAS 9.1, SAS Inc., Cary, NC, USA) before conventional statistical and geostatistical analyses. Data were square root or log transformed if the normality test failed. Conventional statistics [i.e., mean (median for skewed data), standard deviation and coefficient of variation (CV)] were performed to indicate the overall variability for each analyzed item. Correlation matrices for different N forms from both sampling dates, and for relationships between soil moisture, topography, and different N forms at two sampling dates were calculated with the modified test using PASSAGE software (<http://www.passagesoftware.net/>). The modified test corrects the degrees of freedom, based

Spatial patterns of the measured variables were transformed (square root or log-normally) before SV analysis by using GS software (Version 5.1.7, Gamma design software, Plainwell, MI, USA) for Semivariogram (SV hereafter) computation and kriging. We checked the data set to see if any spatial trend of the first- or the second-order existed, and then, before SV computation, we removed the spatial trends from the data set if they existed (Davidson 2002).

SV is a regression model of a series of semivariance values $\gamma(h)$ against the corresponding lag distances h . The semivariance γ at each h is defined as:

$$\gamma(h) = \frac{1}{2N(h)} \sum_{i=1}^{N(h)} [z(i) - z(i+h)]^2, \quad (3)$$

where $N(h)$ is the number of sample pairs separated by lag distance h . $z(i)$ is a measured value at location i . $z(i+h)$ is a measured value at location $i+h$. There are several commonly used SV models, and we chose the model based on three criteria: high minimal extrapolation of semivariance at spatial scale <5 m; and, fitted model shape. The spherical models were chosen in most cases to facilitate the comparison of parameters between variables. The exceptions were NO_3^- and total N in August, and N mineralization and nitrification, for which only the exponential model made the fitted SVs while the spherical model obviously misled (low r^2 and curve misfit). In the computation, the lag distances were chosen as 5 m increments based on sampling scheme (Fig. 1). We compared isotropic and corresponding anisotropic SVs at 0°, 45°, 90°, and 135°, and did not find significant directional patterns. Therefore, isotropic SVs were used. Three SV parameters were derived and used in the analysis: nugget C_0 , range, and the ratio of structure variance C and sill variance $(C + C_0)$ (SH%, hereafter). Nugget reflects either the variability at scales finer than data resolution or random error. Range indicates spatial auto-correlation distance between data pairs. SH% is the proportion of variance due to spatial dependence. SV with a high SH% indicates a strong spatial structure (Brooker 1991; Li and Reynolds 1995). We further carried out krig mapping with calculated SVs for the different N forms. Maps were produced following an ordinary block kriging approach (Davidson 2002) with a block size of 2×2 m². The data that were

Total soil nitrogen (%)

The median of total soil N for both June and August were 0.23% (Table 1), and the standard deviations also remained constant with a value of 0.06. As a consequence, CV was very similar between the two sampling periods with a value of 25 and 26%, respectively, in June and August (Table 1).

The semivariance value was high at the first lag distance for total N in June using spherical model, but after running several possible models such as spherical, exponential, and Gaussian model for the total N data sets in June, we found the parameters did not change much among the different models, nor did the nuggets (data not shown). We reported the results based on spherical model because of the high and good curve shape, also for better comparison of the range values among different N forms. SVs for total soil N in both June and August had high with rather low nugget values. The SH% in both sampling dates were very high (>0.90) (Figs 2d, 3d). The SV range of soil total N was 10.80 m (Fig 2d) in June, and was 10.70 m in August (Fig 3d).

Kriged maps illustrated that soil total N spatial patterns were fairly stable from June to August (Figs. 4d, 5d). The two islands of high values on the lower left and middle part of the kriged map in June reduced in size or disappeared in August.

Available nitrogen

NH_4^+ dominated the total inorganic N pool (Table 1) and determined the spatial distribution of inorganic N in June (Fig. 4a–d). In August, NH_4^+ and NO_3^- were comparable, but soil NO_3^- largely determined the spatial pattern of total inorganic N (Fig. 5a–d).

From June to August, the median of soil NH_4^+ contents increased by 17%, from 17.85 to 20.90 $\mu\text{g/g}$, and the median of soil NO_3^- content increased by 178%, from 6.57 to 18.25 $\mu\text{g/g}$ (Table 1). The standard deviation of NH_4^+ content increased from

Table 1 Summary of statistical parameters of different nitrogen forms, N mineralization, and nitrification, organized by sampling date

Time	Nitrogen Form	<i>n</i>	Mean	Median	SD	CV (%)
June 2000	NH ₄ ⁺ (μg/g)	394	18.99	17.85	7.79	41.00
	NO ₃ ⁻ (μg/g)	394	8.40	6.57	6.50	77.39
	NH ₄ ⁺ + NO ₃ ⁻ (μg/g)	394	27.39	26.43	11.31	41.28
	Total nitrogen (%)	379	0.23	0.23	0.06	24.85
August 2000	NH ₄ ⁺ (μg/g)	387	21.30	20.86	9.21	43.26
	NO ₃ ⁻ (μg/g)	387	20.08	18.25	12.73	63.39
	NH ₄ ⁺ + NO ₃ ⁻ (μg/g)	387	41.37	39.23	17.10	41.34
	Total nitrogen (%)	380	0.24	0.23	0.06	26.36
	N mineralization (μg/g/day)	387	0.22	0.22	0.19	86.36
	Nitrification (μg/g/day)	387	0.19	0.18	0.13	68.42

SD standard deviation

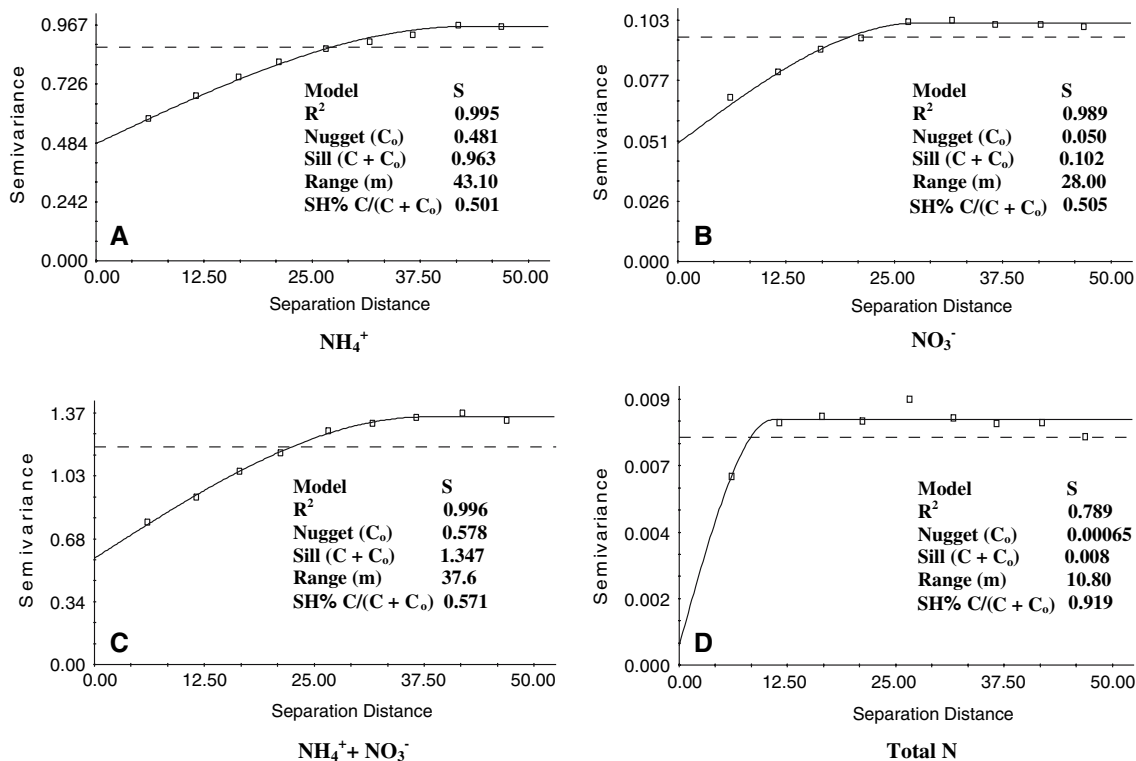


Fig. 2 Semivariograms of NH₄⁺ (a), NO₃⁻ (b), NH₄⁺ + NO₃⁻ (c), and total nitrogen (d) of the whole study site in June 2000. Under the curve is the summary of semivariogram model parameters for different forms of nitrogen. The best model fit to

the data (S = spherical) is indicated. Proportion structural variation $C/(C + C_0)$ is used as an index of the magnitude of spatial dependence. The dash lines indicate the sample variance

7.79 to 9.21 μg/g in 2 months, while that of NO₃⁻ doubled from 6.50 to 12.73 μg/g in the same period (Table 1). However, the CVs of NH₄⁺ at the two

sampling dates were similar (41.00% vs. 43.26% for June and for August, respectively), whereas that of NO₃⁻ decreased from 77.39 to 63.39% (Table

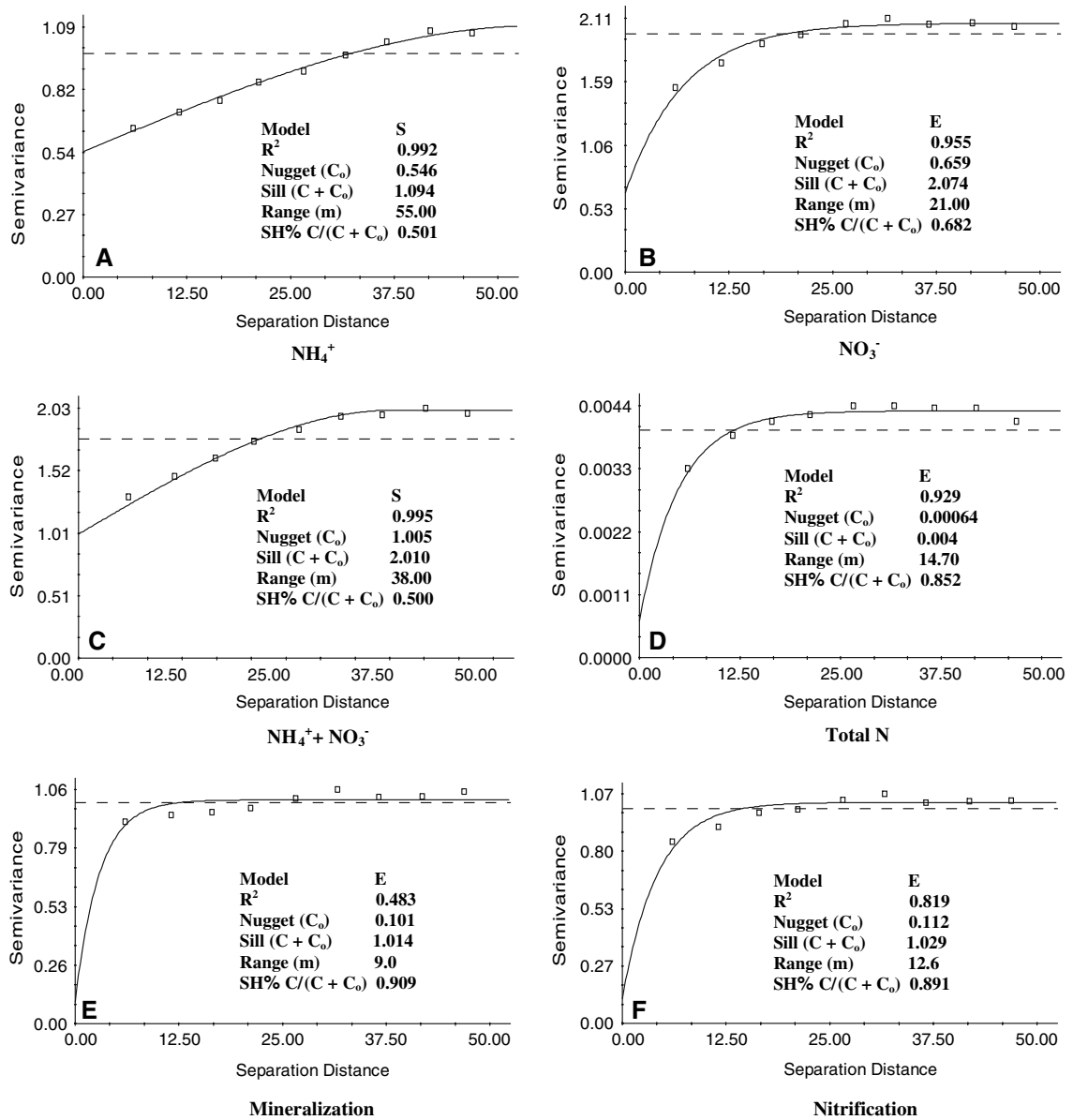


Fig. 3 Semivariograms of NH_4^+ (a), NO_3^- (b), $\text{NH}_4^+ + \text{NO}_3^-$ (c), and total nitrogen (d) of the whole study site in August 2000 and semivariograms of N mineralization (e) and nitrification (f) between June and August 2000. Under the curve is the summary of semivariogram model parameters for mineraliza-

tion and nitrification, and for different forms of nitrogen. The best model fit to the data (E = exponential and S = spherical) is indicated. Proportion structural variation ($C/(C + C_0)$) is used as an index of the magnitude of spatial dependence. The dash lines indicate the sample variance

The SH% for NH_4^+ , NO_3^- , and $\text{NH}_4^+ + \text{NO}_3^-$ were 88, 51, and 53% in June, respectively (Fig. 2c). In August, the SH% of NH_4^+ , NO_3^- , and $\text{NH}_4^+ + \text{NO}_3^-$ were 50, 68, and 57%, respectively.

The SV ranges of NH_4^+ , NO_3^- , and $\text{NH}_4^+ + \text{NO}_3^-$ were 43, 28, and 38 m in June, respectively (Fig. 2g). The SV ranges for all three N forms did not change

much in August with values of 55, 21, and 38 m, respectively (Fig. 3).

When the kriged map of NH_4^+ in August was compared to that of June, the spatial patterns of NH_4^+ differed in the following aspects: (1) patches of high values became larger; (2) the three general north-south direction bands were much more obvious; (3)

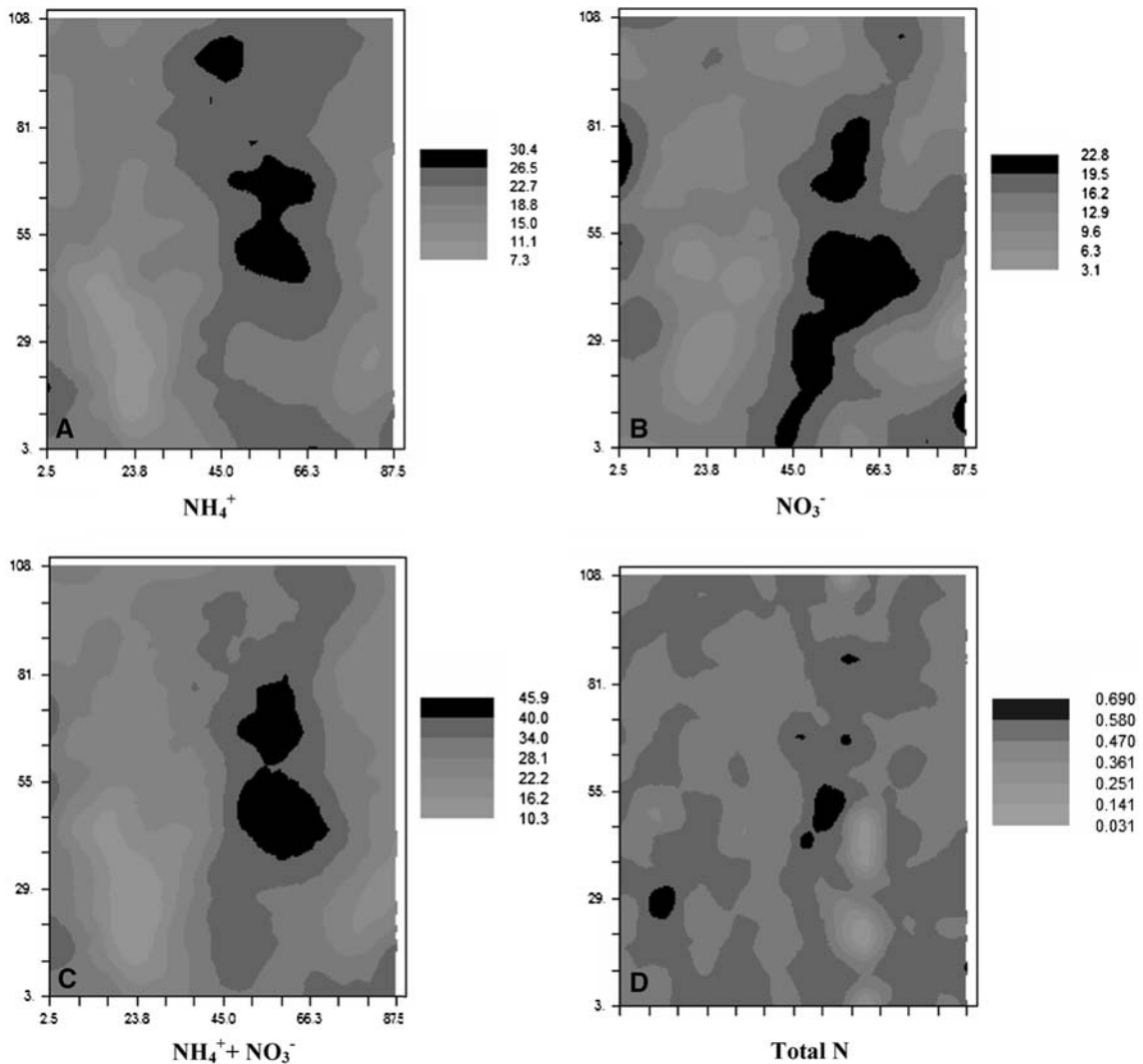


Fig. 4 Distribution of NH_4^+ ($\mu\text{g/g}$) (a), NO_3^- ($\mu\text{g/g}$) (b), $\text{NH}_4^+ + \text{NO}_3^-$ ($\mu\text{g/g}$) (c), and total nitrogen (%) (d) of the whole study site using kriging interpolation in June 2000

less variation within each band in August than in June N mineralization and nitrification (Figs. 4a, 5a). The maps of NQ of August and June showed opposite trends that (1) patches of high Considerable variations in N mineralization and values became smaller in August; (2) the three nitrification were revealed. The net N mineralization general north-south direction bands became less and nitrification were 0.22 and 0.19 $\mu\text{g/g/day}$, obvious; (3) spatial variation within each band was respectively, with standard deviations of 0.19 and higher in August than in June; and (4) islands of 0.13 $\mu\text{g/g/day}$, respectively (Table 6). SVs of both N mineralization and nitrification had moderate values (0.48 and 0.82) with low nugget values and high SH% (Fig. 3e, f). The SV ranges for N mineralization and nitrification were 9.0 and 12.6 m, respectively. However, semivariance values of first lag distance for both processes were quite large (Fig. 3e, f). We also

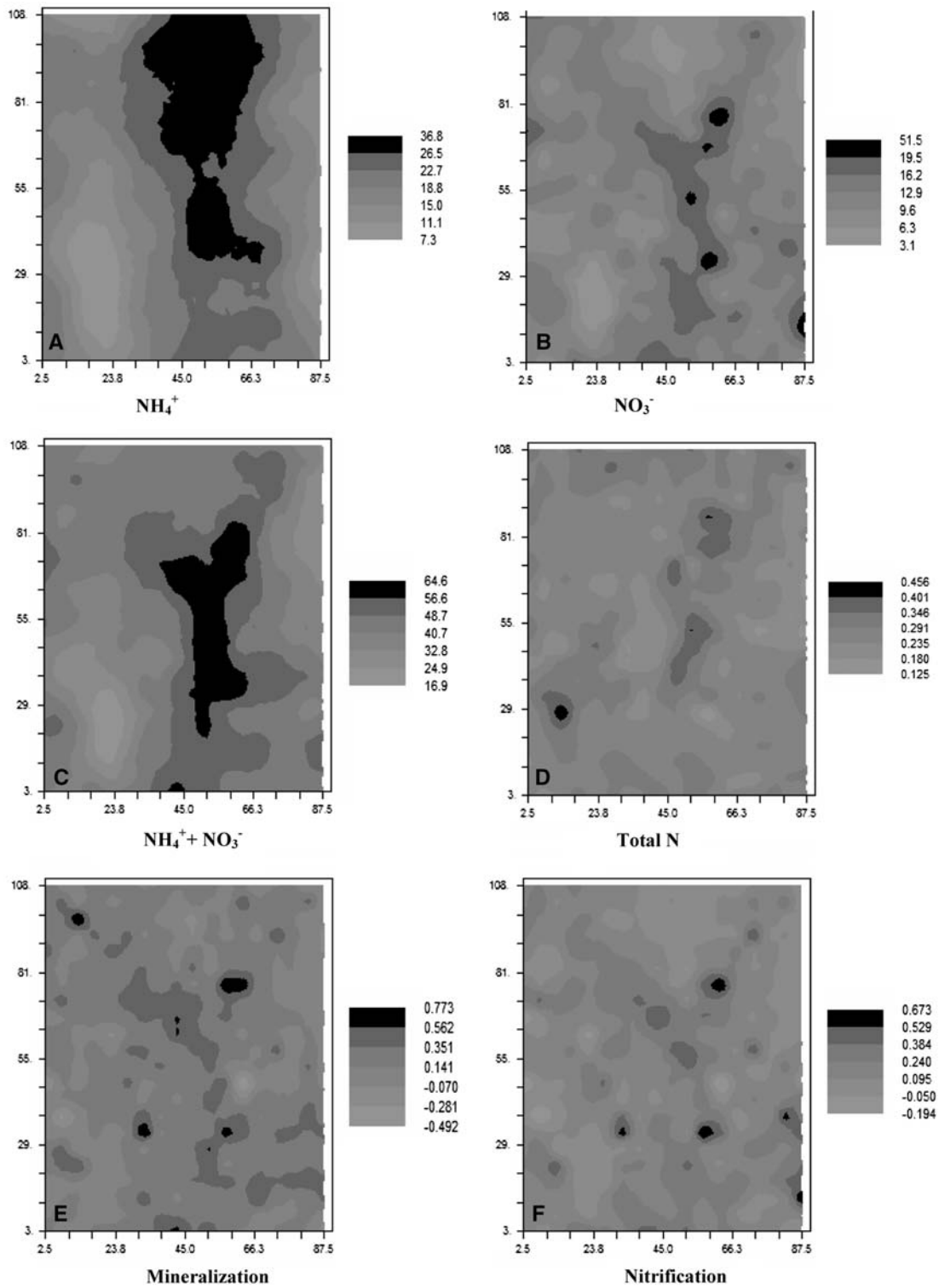


Fig. 5 Distribution of NH_4^+ ($\mu\text{g/g}$) (a), NO_3^- ($\mu\text{g/g}$) (b), $\text{NH}_4^+ + \text{NO}_3^-$ ($\mu\text{g/g}$) (c), and total nitrogen (%) (d) of the whole study site using kriging interpolation in August 2000, and

kriged map of N mineralization ($\mu\text{g/g/day}$) (e) and nitrification ($\mu\text{g/g/day}$) (f) between June and August 2000

applied linear model fitting for N mineralization ($r^2 = 0.83$) and nitrification ($r^2 = 0.68$) to avoid having the calculated parameters an artifact of the model chosen. From the linear model, the values for N mineralization and nitrification were 0.91 and 0.02, respectively; the $C_0 + C$ were 1.06 and 0.03, respectively; the range were both 46.84 m; the SH% were 0.15 and 0.18, respectively. The kriged maps of both processes demonstrated scattered small patches and fine scale variation. The obvious banded patterns shown in the kriged maps of NH_4^+ , NO_3^- , and $\text{NH}_4^+ + \text{NO}_3^-$ did not appear in the maps of N mineralization and nitrification (Fig. 5e, f). There was a significant positive spatial correlation between N mineralization and nitrification ($r = 0.76$ and $P < 0.0001$).

Spatial auto-correlations between different N forms and between times

A number of strong, positive spatial auto-correlations existed among the four different N forms we studied and, for most N forms, existed between June and August (Table 2). Soil total N was positively correlated between the two sampling dates spatially ($r = 0.70$ and $P < 0.0001$). Soil total N was also positively correlated with available N forms spatially (NH_4^+ , NO_3^- , and $\text{NH}_4^+ + \text{NO}_3^-$) in June and August and between June and August ($0.19 < 0.23$ and $P < 0.0001$), except between total N in June and NH_4^+ in August (Table 2). Each available N form (NH_4^+ , NO_3^- , and $\text{NH}_4^+ + \text{NO}_3^-$) was positively correlated with itself spatially between June and August (all > 0.5). They were also positively correlated with each other in June and in August, and between the two sampling dates ($0.24 < 0.85$ and $P < 0.0001$). In addition, $\text{NH}_4^+ + \text{NO}_3^-$ was more spatially correlated to NH_4^+ in June, and more spatially correlated to NO_3^- in August (Table 2).

Correlation between topography, soil moisture and different N forms, N mineralization, and nitrification

Different N forms and topography showed a number of significantly negative correlations including NO_3^- and $\text{NH}_4^+ + \text{NO}_3^-$ in both June and August (Table 3). N mineralization and nitrification were also negatively correlated with topographic position (e.g., N

mineralization and nitrification were generally low on a slope compared to the foothill) (Table 3). Soil moisture, however, was only positively correlated with soil total N in August (Table 3).

Discussion

The total soil N is fairly stable over the 2-month periods as indicated by the constant overall variability (standard deviation and CV). Total soil N remains similar spatial patterns (Fig. 4d, 5d). The two high N islands in the study site were either reduced in size or disappeared from June to August. These indicate that extreme patches in this subtropical forest are more ephemeral than in some other ecosystems, such as the desert system studied by Jackson and Caldwell (1993) where nutrient islands were more pronounced and persistent. The rapid changes in the extreme patches are probably caused by high rates of decomposition, plant uptake, and microbial assimilation. The high SH% values and low nugget values in total soil N (Figs. 2d, 3d) demonstrate that (1) total soil N is highly spatially structured, and (2) that most spatial variations occur at corresponding sampling scales.

In this forest, organic N (total N – available N) overwhelmingly dominate the soil N pool as indicated by the high ratio of total N to available N (50:1 to $> 100:1$; Table 1). The 40–100 times higher standard deviation of total N to that of available N forms, and a high spatial auto-correlation (e.g., SH% value) of soil total N further suggest a strong spatial structure of organic N. The SV ranges of total N (~ 10 m) from this study are similar to what was found in black spruce forest stands in central Alaska (Smithwick et al. 2005). It is higher than that of organic matter found in a desert ecosystem (1.35 m) (Jackson and Caldwell 1993), but smaller than that found in a mature slash pine forest in the southeastern USA (36.2 m) (Lister et al. 2000). The differences may be attributable to the scattered plant clumps in the deserts, and distantly spaced mature overstory pines in southern US pine forests. Our data indicate that the spatial patterning of organic N in ecosystems is highly influenced by the spatial patterns of plant distribution.

The soil NH_4^+ and NO_3^- contents in this forest are within the range found in other forest ecosystems under similar climate conditions (Maithani et al. 1998). The

Table 2 Correlations of NH_4^+ , NO_3^- , $\text{NH}_4^+ + \text{NO}_3^-$, and total N between two sampling periods

		June				August			
		NH_4^+	NO_3^-	$\text{NH}_4^+ + \text{NO}_3^-$	Total N	NH_4^+	NO_3^-	$\text{NH}_4^+ + \text{NO}_3^-$	Total N
June	NH_4^+	1							
	NO_3^-	0.29***	1						
	$\text{NH}_4^+ + \text{NO}_3^-$	0.85***	0.71***	1					
	Total N	0.15**	0.23***	0.23***	1				
August	NH_4^+	0.56***	0.23***	0.53***	0.04	1			
	NO_3^-	0.22***	0.56***	0.45***	0.23***	0.24***	1		
	$\text{NH}_4^+ + \text{NO}_3^-$	0.44***	0.50***	0.60***	0.21***	0.72***	0.82***	1	
	Total N	0.11*	0.22***	0.19***	0.70***	0.17***	0.42***	0.41***	1

The correlations were calculated using a modified test that corrects the degrees of freedom based on the amount of auto-correlation in the data

* $P < 0.05$

** $P < 0.01$

*** $P < 0.001$

Table 3 Correlation between different nitrogen forms and topography (slope position: topographic position was digitized by assigning ridge = 3, back slope = 2, and foothill = 1) and soil moisture at different time, and correlation between N mineralization and nitrification and topography and soil moisture

Time	Nitrogen form	Topography	Moisture
June 2000	NH_4^+ ($\mu\text{g/g}$)	-0.15**	-0.15
	NO_3^- ($\mu\text{g/g}$)	-0.04	-0.21
	$\text{NH}_4^+ + \text{NO}_3^-$ ($\mu\text{g/g}$)	-0.11*	-0.20
	Total nitrogen (%)	-0.03	-0.03
August 2000	NH_4^+ ($\mu\text{g/g}$)	-0.24**	0.11
	NO_3^- ($\mu\text{g/g}$)	-0.11*	0.11
	$\text{NH}_4^+ + \text{NO}_3^-$ ($\mu\text{g/g}$)	-0.20**	0.18
	Total nitrogen (%)	-0.01	0.55*
	N mineralization ($\mu\text{g/g/day}$)	-0.16*	0.06
	Nitrification ($\mu\text{g/g/day}$)	-0.14**	0.06

The correlations were calculated using a modified test, which corrects the degrees of freedom based on the amount of auto-correlation in the data

* $P < 0.05$

** $P < 0.01$

variability of NH_4^+ and NO_3^- were greatly increased from June to August as shown by the increased standard deviations. However, the changes in the content, a feature, which probably facilitates N CVs are small due to more or less proportional changes in means and standard deviations (Table 1). The CVs for NH_4^+ and NO_3^- fall in the range of other observations

(Beckett and Webster 1971; Gross et al. 1995). Gross et al. (1995) found that the CVs of available N ranged from 20 to 133% across the sites of three successional stages and were the largest in the mid-late successional field.

The different SV ranges of NH_4^+ , NO_3^- , and total N suggest that processes responsible for spatial distribution of different N forms may operate at different scales in this forest ecosystem. The fact that the SV ranges of NH_4^+ were higher than that of NO_3^- supports the conclusion from Gallardo et al. (2005) that NH_4^+ tends to have a higher SV range than NO_3^- in different plant communities including grassland, scrubland, shrubland, pine forest, and floodplain forest.

The dominant component which influences spatial patterns of available N shifts from NH_4^+ in June to NO_3^- in August (Figs. 4, 5); although, NH_4^+ quantitatively dominates the inorganic N pool in this ecosystem (Table 1). The spatial pattern of nitrification during the 2-month period may cause this shift (Figs. 4c, 5c, f).

The significant band of high available N in the central right part of the study plot (Figs. 4c, 5c) seems to be affected by the trough topographic feature. The trough soils are deeper and have higher soil moisture (Fig. 5d). The CVs of available N are small due to more or less proportional changes in mineralization and nitrification (Burke 1989; Verchot et al. 2002). However, we do not detect significant correlations between soil moisture and available N

content, N mineralization rate, and nitrification rate (Table 3). Higher sampling intensity of the soil moisture and a map with higher accuracy would help clarify such relationships.

The high nugget values for both NH_4^+ and NO_3^- , consistent with the finding of others (Jackson and Caldwell 1993; Guo et al. 2004), indicate possible finer-scale variations (<5 m) in this area. A nested sampling scheme (multiple scale sampling) covering finer as well as broader scales would be helpful in solving this problem.

Previous research shows that spatial patterns of mineralization and nitrification exist in some ecosystem (Smithwick et al. 2005a), but not in others (Jackson and Caldwell 1993). Our data of mineralization and nitrification generate good SVs with moderate r^2 -values (at least for nitrification Fig. 6f) and high SH%. However, we are reluctant to conclude that our data support the existence of well structured spatial patterns for the two processes due to the high-semivariance values at the first lag distance (Fig. 3e, f). In addition, the SV generated by linear model fitting has much higher r^2 (= 0.83 vs. 0.48 for linear model and spherical model, respectively), for the mineralization process. These evidences demonstrate that the two processes could either be random patterns or have high-fine scale (<5 m) variations. A high-spatial auto-correlation r (= 0.76 and $P < 0.0001$) between the two processes supports the idea that high nitrification occurs where NH_4^+ is readily available (Schlesinger 1997).

The SV of NH_4^+ , NO_3^- , available N, mineralization and nitrification (Fig. 3a–d, f), and their corresponding kriged maps (Fig. 5a–d, f) all indicate finer scale variation. We also find several discrepancies in spatial patterns between mineralization and available N forms (NH_4^+ , NO_3^- , or $\text{NH}_4^+ + \text{NO}_3^-$), as well as between nitrification and available N forms (NH_4^+ , NO_3^- , or $\text{NH}_4^+ + \text{NO}_3^-$). SV of mineralization and nitrification are less spatially structured or are close to the nugget model. The central high value bands that appear in spatial patterns of available N forms (Fig. 5a–d) do not appear in spatial patterns of mineralization and nitrification (Fig. 5e, f). These discrepancies may indicate that mineralization and nitrification rates are less heterogeneous at the broader scale (i.e., at stand level) and that finer-scale processes, such as decomposition and variation in

microbial activity, may control the heterogeneity of available N forms. Plants have significant effects upon N cycling in many ecosystems (e.g., Wedin and Tilman 1990; Epstein et al. 1998; Smithwick et al. 2005b). We could not estimate the role of plant uptake in spatial patterns of available N forms in this system because of the difficulties in quantifying spatial variation of plant N uptake in this study.

From this study, we can generally conclude that in this subtropical secondary evergreen hardwood forest ecosystem: (1) soil total N, NH_4^+ and NO_3^- are all spatially structured at different spatial scales; (2) both NH_4^+ and NO_3^- play roles in establishing the spatial pattern of available N, and alternate their dominance with time; (3) N mineralization and nitrification have either random patterns or high-fine scale (<5 m) variations; (4) N mineralization and nitrification are spatially auto-correlated; and (5) micro-topography affects the spatial patterning of these N forms. Our results indicate that, to better understand the spatio-temporal patterns of N processes and the underlying mechanisms of the observed patterns, multiple samplings with shorter incubation periods and nested sampling methods should be employed. In addition, other processes, such as denitrification and leaching, also need to be monitored.

Acknowledgments The study was funded by the State Key Basic Research and Development Plan of China, National Science Foundation (2000046802-04). We appreciate Dr. Jianguo (Jingle) Wu, Dr. Xinyuan (Ben) Wu, and Dr. Zhengquan Wang for their valuable comments for the earlier draft. We thank Mr. Michael Tuite from Department of Environmental Sciences, University of Virginia for proofreading this manuscript. The strength and clarity of this manuscript were significantly improved by the comments from two anonymous reviewers.

References

- Aber JD, Nadelhoffer KJ, Steudler P, Melillo JM (1989) Nitrogen saturation in northern forest ecosystems. *BioScience* 39:378–386
- Beckett PHT, Webster R (1971) Soil variability: a review. *Soil Fertil* 34:1–15
- Binkley D, Hart SC (1989) The components of nitrogen availability assessments in forest soils. *Adv Soil Sci* 10:57–112
- Brady NC, Weil RR (1999) The nature and properties of soil 12th ed. Prentice Hall, Upper Saddle River, USA
- Bremner JM (1996) Nitrogen-total. In: Sparks DL (eds) Methods of soil analysis. Part 3. Chemical methods. Soil

- Science Society of America, and American Society of Agronomy, Madison, Wisconsin, USA, pp 1085–1088
- Brooker PI (1991) A geostatistical primer. World Scientific Publishing, Singapore
- Burke IC (1989) Control of nitrogen mineralization in a sagebrush steppe landscape. *Ecology* 70:1115–1126
- Cain ML, Subler S, Evans JP, Fortin MJ (1999) Sampling spatial and temporal variation in soil nitrogen availability. *Oecologia* 118:397–404
- Cassidy TM, Fownes JH, Harrington RA (2004) Nitrogen limits an invasive perennial shrub in forest understorey. *Biol Inv* 6(1):113–121
- Chen C (2000a) The Dujiangyan region-pivot sector of assemblage, differentiation and maintenance of biodiversity in northern part of Hengduan mountain. *Acta Ecol Sin* 20:28–34 (in Chinese with English summary)
- Chen C (2000b) Biodiversity research and conservation of Dujiangyan, China. Sichuan Science and Technology Press, Sichuan, China
- Cowling SA, Field CB (2003) Environmental control of leaf area production: implications for vegetation and land-surface modeling. *Glob Biogeochem Cy* 17(1):1007. doi:10.1029/2002GB001915
- Davis JC (2002) Statistics and data analysis in geology, 3rd edn. Wiley, New York
- Epstein HE, Burke IC, Mosier AR (1998) Plant effects on spatial and temporal patterns of nitrogen cycling in shortgrass steppe. *Ecosystems* 1(4):374–385
- Gallardo A, Rodriguez-Saucedo JJ, Covelo F, Fernandez-Ales R (2000) Soil nitrogen heterogeneity in a Dehesa ecosystem. *Plant Soil* 222:71–82
- Gallardo A, Paramor R, Covelo F (2005) Soil Ammonium vs. nitrate spatial pattern in six plant communities: simulated effect on plant populations. *Plant Soil* 277:207–219
- Gardner WH (1986) Water content. In: Klute A (ed) Methods of soil analysis. Part 1. Physical and mineralogical methods. American Society of Agronomy, and Soil Science Society of America, Madison, Wisconsin, USA, pp 493–494
- Garten CT Jr, Huston MA, Thoms CA (1994) Topographic variation of soil nitrogen dynamics at Walker branch watershed, Tennessee. *For Sci* 40:497–512
- Gross KL, Pregitzer KS, Burton AJ (1995) Spatial variation in nitrogen availability in three successional plant communities. *J Ecol* 83:357–367
- Guo D, Mou P, Jones RH, Mitchell RJ (2004) Spatio-temporal patterns of soil available nutrients following experimental disturbance in a pine forest. *Oecologia* 138:613–621
- Hammer RD, O'Brien RG, Lewis RJ (1987) Temporal and spatial soil variability on three forested landtypes on the mid-Cumberland Plateau. *Soil Sci Soc Am J* 51:1320–1326
- Hutchings MJ, John EA, Wijesinghe DK (2003) Toward understanding the consequences of soil heterogeneity for plant populations and communities. *Ecology* 84(9):2322–2334
- Jackson RB, Caldwell MM (1993) Geostatistical pattern of soil heterogeneity around individual plants. *J Ecol* 81:683–692
- Kimmins JP (2004) Forest ecology: a foundation for sustainable forest management and environmental ethics in forestry. Pearson Prentice Hall, Upper Saddle River, NJ, USA
- Kronzucker HJ, Siddiqi MY, Glass AD (1997) Conifer roots discrimination against soil nitrate and the ecology of forest succession. *Nature* 385:59–61
- Lane DR, Bassirrad H (2005) Diminishing spatial heterogeneity in soil organic matter across a prairie restoration chronosequence. *Restor Ecol* 13(2):403–412
- Li HR, Reynolds JF (1995) On the quantification of spatial heterogeneity. *Oikos* 73:280–284
- Lister AJ, Mou P, Jones RH, Mitchell RJ (2000) Spatial patterns of soil and vegetation in a 40-year-old slash pine (*Pinus elliottii* Engelm.) forest in the Coastal Plain of South Carolina, USA. *Can J For Res* 30:145–155
- Lovett GM, Rueth H (1999) Soil nitrogen transformations in beech and maple stands along a nitrogen deposition gradient. *Ecol Appl* 9:1330–1344
- Maithani K, Arunachalam A, Tripathi RS, Pandey HN (1998) Influence of leaf litter quality on N mineralization in soils of subtropical humid forest regrowths. *Biol Fertil Soils* 27(1):44–50
- Maynard DG, Kalra YP (1993) Nitrate and exchangeable ammonium nitrogen. In: Carter MR (eds) Soil sampling and methods of analysis. Lewis Publishers, Boca Raton, FL, USA, pp 25–34
- Morris SJ, Boerner REJ (1998) Landscape patterns of nitrogen mineralization and nitrification in southern Ohio hardwood forests. *Landsc Ecol* 13:215–224
- Mou P, Mitchell RJ, Jones RH (1993a) Ecological field theory model: a mechanistic approach to simulate plant-plant interactions in southeastern forest ecosystems. *Can J For Res* 23:2180–2193
- Mou P, Fahey TJ, Hughes JW (1993b) Nutrient accumulation in vegetation following whole-tree harvest of a northern hardwood ecosystem. *J Appl Ecol* 30:661–675
- Mou P, Jones RH, Guo D, Lister A (2005) Regeneration strategies, disturbance and plant interactions as organizers of vegetation spatial patterns in a pine forest. *Landsc Ecol* 20:971–987
- Perez CA, Hedin LO, Armesto JJ (1998) Nitrogen mineralization in two unpolluted old-growth forests of contrasting biodiversity and dynamics. *Ecosystems* 1(4):361–373
- Raison RJ, Connell MJ, Khanna PK (1987) Methodology for studying fluxes of soil mineral-N in situ. *Soil Biol Biochem* 19:521–530
- Rastetter EB, Agren GI, Shaver GR (1997) Response of N-limited ecosystems to increased CO₂: a balanced-nutrition, coupled-element-cycles model. *Ecol Appl* 7(2):444–460
- Reich PB, Hobbie SE, Lee T, Ellsworth DS, West JB, Tilman D, Knops JMH, Naeem S, Trost J (2006) Nitrogen limitation constrains sustainability of ecosystem response to CO₂. *Nature* 440:922–925
- Schlesinger WH (1997) Biogeochemistry: an analysis of global change, 2nd edn. Academic, New York
- Siemann E, Rogers WE (2003) Changes in light and nitrogen availability under pioneer trees may indirectly facilitate tree invasions of grasslands. *J Ecol* 91(6):923–931
- Smithwick EAH, Mack MC, Turner MG, Chapin FS III, Zhu J, Balser TC (2005a) Spatial heterogeneity and soil nitrogen

- dynamics in a burned black spruce forest stand: distinct controls at different scales. *Biogeochemistry* 76:517–537
- Smithwick EAH, Turner MG, Metzger KL, Balsler TC (2005b) Variation in NH_4^+ mineralization and microbial communities with stand age in lodgepole pine (*Pinus contorta*) forests, Yellowstone National Park (USA). *Soil Biol Biochem* 37(8):1546–1559
- Tamm CO (1991) Nitrogen in terrestrial ecosystems. Springer, Berlin Heidelberg
- Upadhaya K, Pandey HN, Law PS, Tripathi RS (2005) Dynamics of fine and coarse roots and nitrogen mineralization in a humid subtropical forest ecosystem of northeast India. *Biol Fertil Soils* 41(3):144–152
- Verchot LV, Groffman PM, Frank DA (2002) Landscape versus ungulate control of gross mineralization and gross nitrification in semi-arid grasslands of Yellowstone National Park. *Soil Biol Biochem* 34:1691–1699
- Wedin DA, Tilman D (1990) Species effects on nitrogen cycling: a test with perennial grasses. *Oecologia* 84:433–441
- Wijesinghe DK, John EA, Hutchings MJ (2005) Does pattern of soil resource heterogeneity determine plant community structure? An experimental investigation. *J Ecol* 93:99–112